

A. Abbou<sup>1</sup>,  
T. Nasser<sup>2</sup>,  
H. Mahmoudi<sup>1</sup>,  
M. Akherraz<sup>1</sup>,  
A. Essadki<sup>2</sup>

J. Electrical Systems 8-3 (2012): 317-327

**dSPACE IFOC Fuzzy Logic Controller  
Implementation for Induction Motor  
Drive**



This paper presents an dSPACE implementation of a sensorless speed control for three-phase squirrel-cage induction motor control using Indirect Field Oriented control (IFOC) technique. The speed loop regulation is carried out by a fuzzy controller giving exceeding performance in comparison with a classic PI regulator. The design of the controller is based on the experience without knowing the mathematical model of the Motor. Experimental results for a 3kW induction motor are presented and analyzed using a dSPACE system with DS1104 controller board based on digital processor Texas Instruments TMS320F240 DSP. A good agreement between the simulation results and experimental results are achieved.

Keywords: dSPACE, IFOC, Induction Motor (IM), PI fuzzy, Sensorless.

## 1. Introduction

The induction motor is one of the most widely used machines in industrial applications due to its high reliability, relatively low cost, and modest maintenance requirements. The Rotor Flux Oriented Control (RFOC) is probably the most common control method used for high-performance induction machine applications. Rotor flux orientation (RFO) in the synchronous reference frame is considered here [1]-[2]. There are other orientation possibilities, but rotor flux orientation is the most prominent. The RFOC method involves making the induction machine behave similarly to a DC machine. The rotor flux is aligned entirely along the  $d$ -axis. The stator currents are split into two components: a Field-producing component that induces the rotor flux and a torque-producing component that is orthogonal to the rotor field. This is analogous to the DC machine where the field flux is along one direction, and the commutator ensures an orthogonal armature current vector [4]. This task is greatly simplified through transformation of the machine variables to the synchronously rotating reference frame.

On the other hand, ongoing research has concentrated on the elimination of the speed sensor at the machine shaft without deteriorating the dynamic performance of the drive control system [5]-[6]-[9]. The advantages of speed sensorless induction motor drives are reduced hardware complexity and lower cost, reduced size of the drive machine, elimination of the sensor cable, better noise immunity, increased reliability and less maintenance requirements.

In this paper we interest a real implementation using DS1104 controller board of indirect rotor flux oriented control (IRFOC) of an induction motor supplied by hysteresis current-controlled inverter. Simulation and Experimental results of a sensorless speed control using a PI Fuzzy speed controller are presented. The control loop of the motor speed, proposed in this paper, is provided by a PI controller based on fuzzy logic. The induction motor speed estimation proposed in this paper is based on simple relationships between voltage and current and easy to implement in real time.

\* Corresponding author: A. Abbou, Ecole Mohammadia d'Ingénieurs, Avenue Ibn Sina BP 765, Madinat Al Irfane 10100, Agdal Rabat Morocco, E-mail: [abbou@emi.ac.ma](mailto:abbou@emi.ac.ma)

<sup>2</sup> ENSET Avenue de l'Armée Royal, Agdal Rabat Morocco

This paper organized as follows: The induction model is presented in the second section, the RFOC strategy is developed in the third section, section fourth present a speed method estimation, the speed PI Fuzzy controller design is performed in the five section, and section six is devoted to experimental setup and results, a conclusion and reference list end the paper

## 2. Induction motor model

The state equation of induction motor written in the (d, q) oriented axes, can be expressed as follows [5]:

$$\begin{cases} \dot{x} = f(x) + g(x).u(t) \\ y(t) = h(t) \end{cases} \quad (1)$$

Where  $x = [i_{sd} \quad i_{sq} \quad \Phi_{rd} \quad \Omega]^t$  and  $u = [V_{sd} \quad V_{sq}]^t$  are respectively the state vector and the control vector.

With:

$$f(x) = \begin{bmatrix} f_1(x) \\ f_2(x) \\ f_3(x) \\ f_4(x) \end{bmatrix} = \begin{bmatrix} -\gamma i_{sd} + k \mu \Phi_{rd} + p \Omega i_{sq} + Mk \frac{i_{sq}^2}{\Phi_{rd}} \\ -\gamma i_{sq} - \mu \Omega \Phi_{rd} - p \Omega i_{sd} - Mk \frac{i_{sq} i_{sd}}{\Phi_{rd}} \\ -k \Phi_{rd} + Mk i_{sd} \\ \eta \Phi_{rd} i_{sq} \frac{C_r}{J} \end{bmatrix} \quad (2)$$

$$h = [\Omega \quad \Phi_{rd}]^t \quad (3) \quad g = \begin{bmatrix} \delta & 0 & 0 & 0 \\ 0 & \delta & 0 & 0 \end{bmatrix} \quad (4)$$

$$\text{And } \gamma = (R_s + (\frac{M}{L_r})^2 . R_r) . \delta = R_{sr} . \delta, \quad k = \frac{R_r}{L_r}, \quad (5)$$

$$\mu = \frac{M}{\sigma L_s L_r} \quad \eta = \frac{pM}{J L_r}, \quad \delta = \frac{1}{\sigma L_s}, \quad a = \frac{M}{L_r}, \quad \sigma = 1 - \frac{M^2}{L_s L_r}, \quad (6)$$

The electromagnetic torque can be expressed as ( $\Phi_{rq}=0$ ):

$$C_e = p \frac{M}{L_r} (\Phi_{rd} . i_{sq} - \Phi_{rq} . i_{sd}) = p \frac{M}{L_r} \Phi_{rd} . i_{sq} \quad (7)$$

With,

$V_{sd,q}$  : Stator voltage in the stationary d, q axis

$i_{sd,q}$  : Stator current in the stationary d, q axis

$\Phi_{rd,q}$  : Rotor flux in the stationary d, q axis

$\Omega$  : Rotor speed

$\omega_r$  : Rotor electrical speed

- $\rho$  : Rotor flux angle
- $\sigma$  : Leakage coefficient of the machine
- $C_r$  : Load torque
- $J$  : Rotor inertia
- $p$  : Number of pole pairs
- $R_s$  : Stator resistance
- $R_r$  : Rotor resistance
- $M, L_s, L_r$  : Are respectively the mutual, the stator and the rotor cyclic inductances

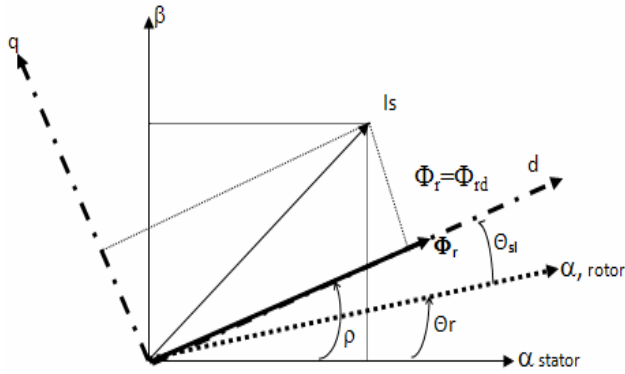


Fig.1. d-q and  $\alpha$ - $\beta$  frames

### 3. RFOC Scheme for Induction Motor

#### a. IRFOC Strategy

The block diagram of the proposed sensorless control scheme is shown in figure 2 is similar to that of the separately excited DC machine. The space angle of the rotor flux space phasor ( $\rho$ ) is obtained as the sum of the rotor angle ( $\theta_r$ ) and the reference value of the slip angle ( $\theta_{sl}$ ). These angles are shown in Fig.1 and the stator voltage angular frequency ( $\omega_s$ ) is determined by the controller [2] according to which the speed of the rotor flux space phasor, is

$$\omega_s = \omega_r + \omega_{sl} \tag{8}$$

Where  $\omega_r$  is the rotor electrical speed,

$$\omega_r = \frac{d\theta_r}{dt} \tag{9}$$

And  $\omega_{sl}$  is the reference value of the slip frequency, 
$$\omega_{sl} = \frac{M \cdot i_{sq}}{T_r \cdot \Phi_{rd}} \tag{10}$$

Furthermore, 
$$\omega_s = \frac{d\rho}{dt}, \tag{11}$$

Thus the rotor flux angle is given by 
$$\rho = \theta_r + \int \frac{M \cdot i_{sq}}{T_r \cdot \Phi_{rd}} dt \tag{12}$$

Note that the rotor pole position is not absolute, but is slipping with respect to the rotor at frequency  $\omega_{sl}$ . The phasor diagram suggests that for decoupling control, the stator flux

component of current  $i_{s\alpha}$  should be aligned and the  $d$  axis, and the torque component of current  $i_{s\beta}$  should be on the  $q$  axis, as shown.

In order to transform the two rotating input quantities into two stationary output quantities, we need to perform the inverse Park transformations  $P(\rho)$ . It utilizes the positional angle of the rotor flux ( $\rho$ ) to do this:

$$\begin{bmatrix} i_{s\alpha} \\ i_{s\beta} \end{bmatrix} = \begin{bmatrix} \cos \rho & -\sin \rho \\ \sin \rho & \cos \rho \end{bmatrix} \begin{bmatrix} i_{sd} \\ i_{sq} \end{bmatrix} \quad (13)$$

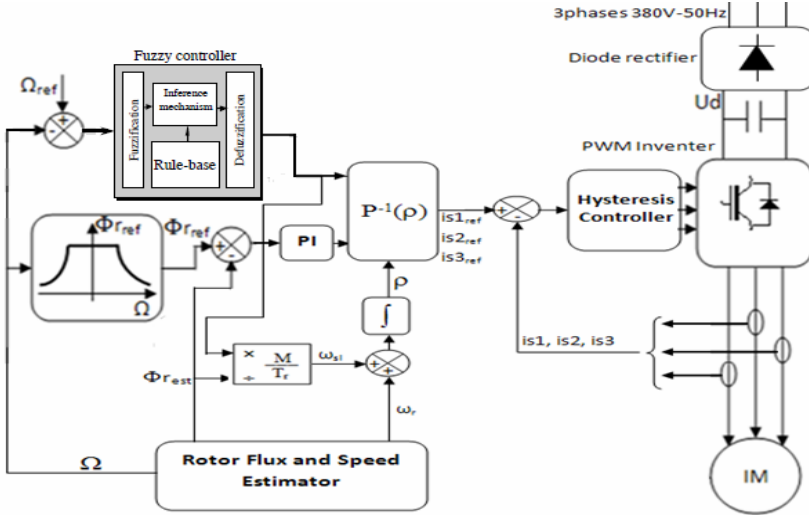


Fig.2. Block diagram of sensorless control proposed

### b. Rotor flux estimation

The rotor flux components can be synthesized more easily with the help of speed and current signals. The rotor circuit equations of ( $\alpha, \beta$ ) equivalent circuits [2] can be given as.

$$\begin{cases} \frac{d\Phi_{r\alpha}}{dt} + p\Omega \cdot \Phi_{r\beta} + R_r \cdot i_{r\alpha} = 0 \\ \frac{d\Phi_{r\beta}}{dt} - p\Omega \cdot \Phi_{r\alpha} + R_r \cdot i_{r\beta} = 0 \end{cases} \quad (14)$$

Adding terms  $M \cdot k \cdot i_{s\alpha}$  and  $M \cdot k \cdot i_{s\beta}$ , respectively, on both sides of the above equations, we get

$$\begin{cases} M \cdot k \cdot i_{s\alpha} = \frac{d\Phi_{r\alpha}}{dt} + k(M \cdot i_{s\alpha} + L_r \cdot i_{r\alpha}) + p\Omega \Phi_{r\beta} \\ M \cdot k \cdot i_{s\beta} = \frac{d\Phi_{r\beta}}{dt} + k(M \cdot i_{s\beta} + L_r \cdot i_{r\beta}) - p\Omega \Phi_{r\alpha} \end{cases} \quad (15)$$

Substituting equations (16) and (17), respectively, and simplifying, we get:  $\Phi_{r\alpha} = M \cdot i_{s\alpha} + L_r \cdot i_{r\alpha}$

(16)

$$\Phi_{r\beta} = M \cdot i_{s\beta} + L_r \cdot i_{r\beta}$$

(17)

$$\begin{cases} \frac{d\Phi_{r\alpha}}{dt} = k.M.i_{s\alpha} - p\Omega\Phi_{r\beta} - k.\Phi_{r\alpha} \\ \frac{d\Phi_{r\beta}}{dt} = k.M.i_{s\beta} + p\Omega\Phi_{r\alpha} - k.\Phi_{r\beta} \end{cases} \quad (18)$$

Equation (18) gives rotor fluxes as functions of stator currents and speed. Therefore, knowing these signals, the fluxes and corresponding unit vector signals can be estimated. Finally,

$$\Phi_r = \sqrt{(\Phi_{r\alpha}^2 + \Phi_{r\beta}^2)} \quad (19)$$

#### 4. Speed Method Estimation

The estimation speed method used for induction motor is simple and can be easily implemented. It is possible to obtain an expression for the rotor speed by considering the following equation:

$$\hat{\omega} = \omega_s - \omega_r \quad (20)$$

Where  $\omega_s$  is the speed of the rotor flux (relative to the stator):

$$\omega_s = \frac{d\rho}{dt} \quad (21)$$

And  $\omega_r$  the angular slip frequency, given by equation:

$$\omega_r = \frac{R_r}{p} \frac{C_e}{|\Phi_r|^2} \quad (22)$$

In order words,  $\omega_s$  is the speed of the rotor flux linkage space vector with respect to the rotor. It is possible to obtain an expression for  $\omega_s$  in terms of the rotor linkage components by expanding the expression for the derivative (14). Since the rotor flux linkage space vector expressed in the stationary reference frame is:

$$\rho = \text{Arctg} \left( \frac{\Phi_{r\beta}}{\Phi_{r\alpha}} \right) \quad (23)$$

$$\omega_s = \frac{d\rho}{dt} = \frac{(\Phi_{r\alpha} \dot{\Phi}_{r\beta} - \Phi_{r\beta} \dot{\Phi}_{r\alpha})}{(\Phi_{r\alpha}^2 + \Phi_{r\beta}^2)} \quad (24)$$

Considering the electromagnetic expression, the angular slip frequency can be rewritten as:

$$\omega_r = \frac{R_r}{p} \frac{C_e}{|\Phi_r|^2} = \frac{M}{T_r} \frac{(\Phi_{r\alpha} i_{s\beta} - \Phi_{r\beta} i_{s\alpha})}{(\Phi_{r\alpha}^2 + \Phi_{r\beta}^2)} \quad (25)$$

In this last case, the components of stator flux are thus known for the control of the machine. We will make use of it, as well as equations (2) binding flux to the currents, to determine the components of rotor flux:

$$\begin{cases} \Phi_{r\alpha} = \frac{L_r}{M} (\Phi_{s\alpha} - \sigma L_s i_{s\alpha}) \\ \Phi_{r\beta} = \frac{L_r}{M} (\Phi_{s\beta} - \sigma L_s i_{s\beta}) \end{cases} \quad (26)$$

### 5. PI Fuzzy Controller

The block diagram of the PI Fuzzy controller is shown in fig.3,

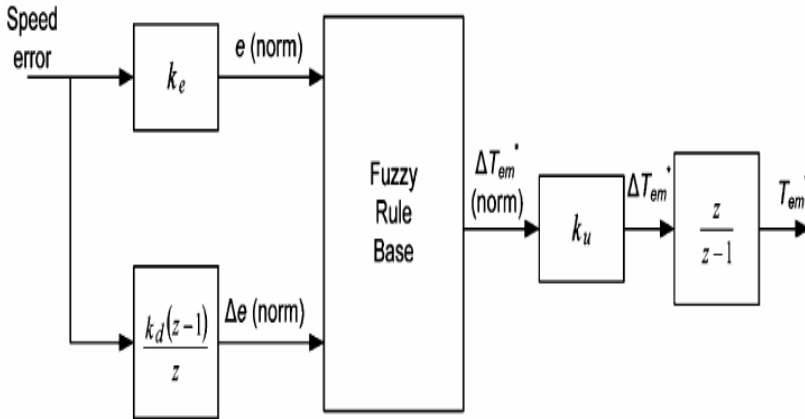


Fig.3. PI Fuzzy controller

FLC replace the traditional PI controller. For the proposed FL speed controller, the inputs are the normalized values of the speed error and the rate of change to remain between  $\pm 1$  limits of speed error. Two scaling factors ( $K_e$  and  $K_d$ ) are used to normalize the actual speed error and its rate of change. The output of the controller is the normalized change of the motor torque command which when multiplied by a third scaling factor ( $K_u$ ) generates the actual value of the rate of change of the motor torque demand.

Finally, a discrete integration is performed to get the value of the electromagnetic torque command. Hence a PI-Type FLC is created [13]. The FLC structure is shown in Fig. 3.

Table I shows the fuzzy rule base with 49 rules which can be obtained from observation of the drive performance at different operating points [13].

The following fuzzy sets are used:

- NB**=NEGATIVE BIG,
- NM**=NEGATIVE MEDUIM,
- NS** =NEGATIVE SMALL,
- EZ** = ZERO,
- PS** = POSITIVE SMALL,
- PM**= POSITIVE MEDUIM,
- PB** = POSITIVE BIG.

The membership functions of the FLC shown in Fig. 4 are obtained by a trial and error technique where the EZ fuzzy set has a narrow shape different from other fuzzy sets to improve the controller steady state performance.

The Fuzzy controller input and output membership function (a) speed error (e), (b) change in speed error ( $\Delta e$ ) and (c) change in the torque command are given in following figure:

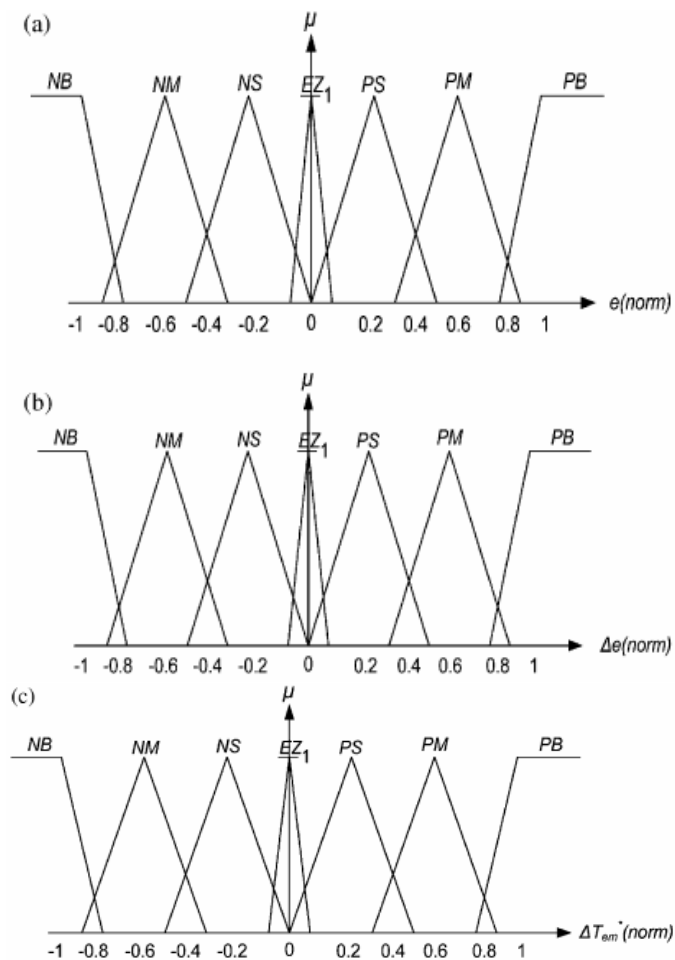


Fig. 4. Membership functions

TABLE I  
FUZZY RULES BASES

$e_{\omega}$	NB	NM	NS	EZ	PS	PM	PB
$\Delta e_{\omega}$							
PB	EZ	PS	PM	PB	PB	PB	PB
PM	NS	EZ	PS	PM	PB	PB	PB
PS	NM	NS	EZ	PS	PM	PB	PB
EZ	NB	NM	NS	EZ	PS	PM	PB
NS	NB	NB	NM	NS	EZ	PS	PM
NM	NB	NB	NB	NM	NS	EZ	PS
NB	NB	NB	NB	NB	NM	NS	EZ

For example, it follows from Table I that the first rule is:

IF  $e$  is NB and  $\Delta e$  is PB then  $\Delta T_e$  is EZ

On every of these universes is placed seven triangular membership functions (fig.6). It was chosen to set these universes to normalized type for all of inputs and output. The range of universe is set to -1 to 1.

## 6. Experimental Setup and Results

The control algorithm has been implemented using a dSPACE board with TMS320F240 DSP. The dSPACE works on Matlab/Simulink platform which is a common engineering software and easy to understand. Another feature of the dSPACE is the Control desk which allows the graphical user interface, through the control desk the user can observe the response of the system also he can give command to the system through this interface. Real time interface is needed for the dSPACE to work. Real-time Interface (RTI) is the link between dSPACE's real-time systems and the development software MATLAB/Simulink from the Math Works. It extends Real-Time Workshop (C-code generation) for the seamless and automatic implementation of our Simulink Models on the dSPACE Real-time Hardware. This allows us to concentrate fully on the actual design process and to carry out fast design iterations. To specify a dSPACE I/O board, we can simply pick up the corresponding I/O module graphically from the RTI block library and then attach and parameterize it within simulink.

Power circuit for the drive consist a Semikron IGBT based voltage source inverter with opto-isolation and gate driver circuit SKHI22A. The dc voltage for the VSI is achieved through a three-phase diode bridge rectifier module. A capacitive filter is used at the dc link of this module to reduce the voltage ripples.

The motor used in this experimental investigation is a three phases, 3KW, 4 poles squirrel cage induction machine, 7.2A/12.5A, 220V/380V, 50HZ and 1400rpm.

The induction motor is driven by IRFOC algorithm included in a speed control closed-loop and run under different loads with the help of DC generator mechanically coupled to the motor and having the following characteristics: 3KW, 120V, 25A and 1500rpm.

All current and voltage are measured using LEM sensors (LEM HX15-P, LEM LV25-P), and both of them are then transformed to be a voltage ranging from 0 to  $\pm 10$  volts which will be the input of A/D respectively.

Figure 5 gives the experimental platform scheme used:

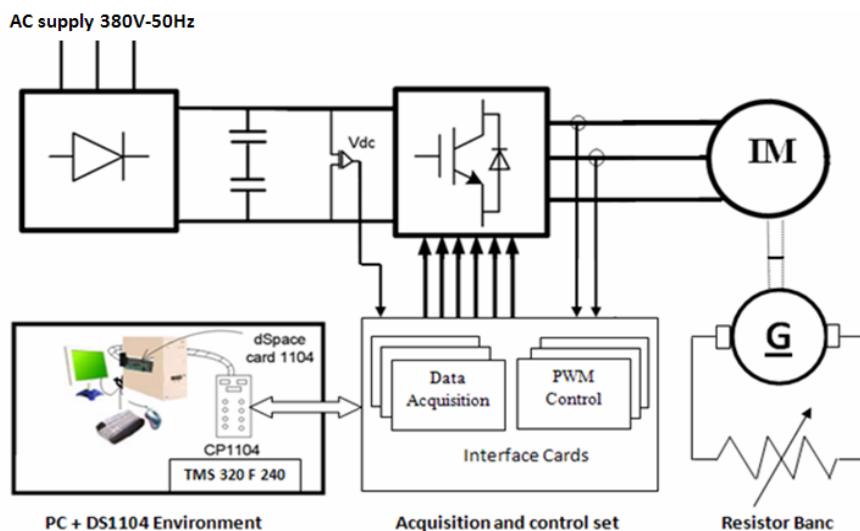
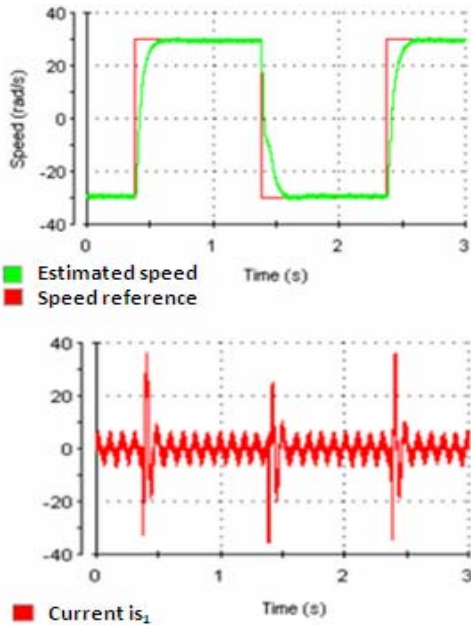


Fig. 5. Experimental test setup.

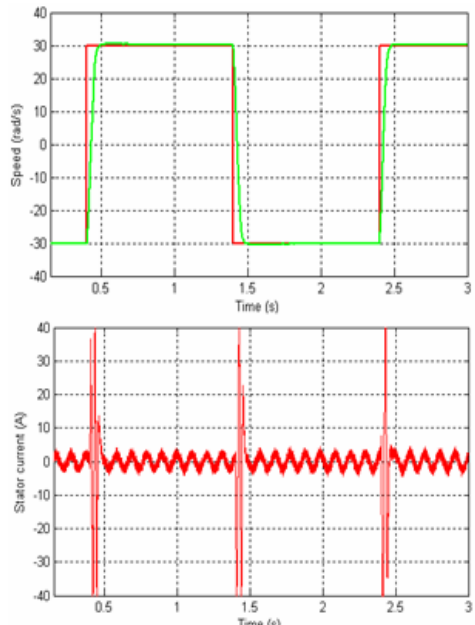
The torque value is considered equal to zero in the first test, but for the second test, the load torque is 10Nm.



A- Functioning in low speed ( $\pm 30\text{rad/s}$ )

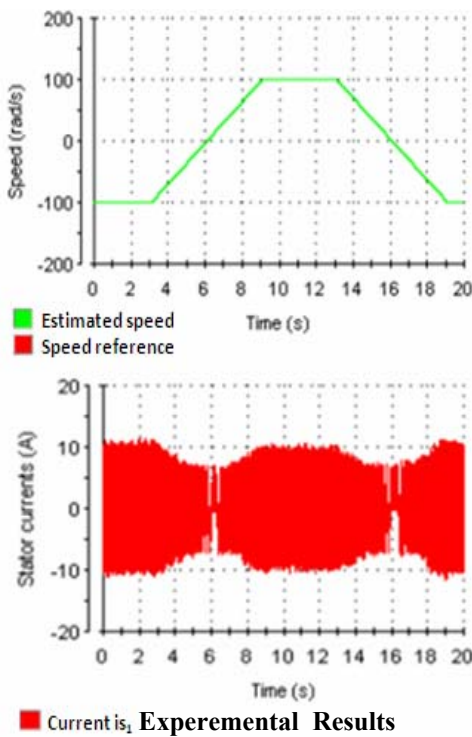


Experimental Results

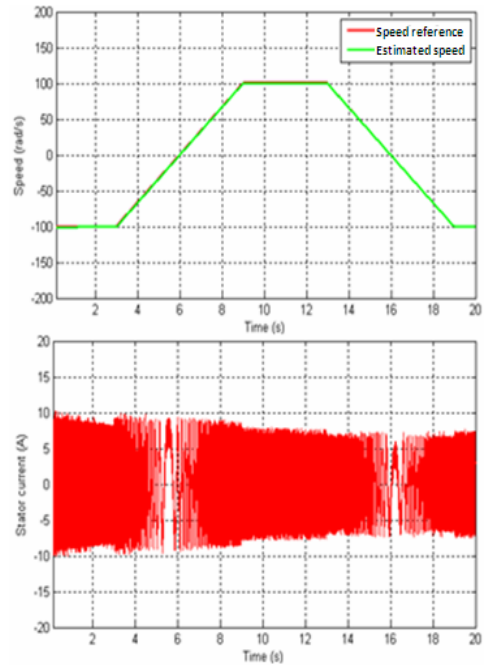


Simulation Results

B- Functioning when the speed change ( $\Omega = \pm 100\text{rad/s}$ )



Experimental Results



Simulation Results

Fig. 6. Experimental Results

### C. Commentaries'

The results presented in figure 6 show a perfect correlation between experiment based on the dSPACE board with TMS320F240 DSP and simulation using Matlab/Simulink, for the planned operation (low speed and when the speed change). Estimated speed follows the reference speed closely. The stator phase current in the induction motor remains sinusoidal and takes appropriate value.

## 7. Conclusion

This paper presents a comparison between experimental and simulation results of an efficient Sensorless speed Indirect Field oriented Control for a 3kw induction motor drives. The results were satisfactory and the proposed PI fuzzy controller gives the system good performance and good dynamic behavior even at low speed. Also, the estimated speed follows the reference speed closely. Good agreement between theory and experiment is obtained by using a dSPACE system with DS1104 controller board based on digital processor Texas Instruments TMS320F240 DSP.

## Appendix

TABLE II  
PARAMETERS INDUCTION MOTOR

Rated power	3 KW
Voltage	380V Y
Frequency	50 Hz
Pair pole	2
Rated speed	1400 rpm
Stator resistance	1.7 $\Omega$
Rotor resistance	2.68 $\Omega$
Inductance stator	229 mH
Inductance rotor	229 mH
Mutual inductance	217 mH
Moment of Inertia	0.046 kg.m <sup>2</sup>

## References

- [1] B.Nahid-Mobarakeh, F. Betin, D. Pinchon and G.A. Capolino, Sensorless field oriented control of induction machines using a reduced order linear disturbance observer, *Electromotion*, Marrakesh, vol. 10, pp. 545–550, Oct. 2003.
- [2] J. Holtz, Sensorless Control of induction motor drives, *Proc.IEEE*, vol. 90, n°8, pp.1359-1394, 2002.
- [3] Abbou A. and Mahmoudi H. ,Real Time Implementation of a Sensorless Speed Control of Induction Motor using DTFC Strategy, Proceedings of the International Conference on Multimedia Computing and Systems ICMCS'09, pp.327-333, Ouarzazate, Morocco, April 2-4, 2009.
- [4] D.Casadei,F. Profumo, G.Serra and A. Tani, FOC and DTC: Tox viable schemes for induction motors Torque control, *IEEE Trans. Power Electronics*, vol. 17, n° 5, Sept 2002.

- [5] B. K. Bose, *Modern Power Electronics and AC Drives*, (Pearson Education, Inc. 2002).
- [6] M. Hinkkanen, Analysis and design of full-order flux observers for sensorless induction motors, *IEEE Trans. Ind. Electron.*, vol. 51, no. 5, pp. 1033–1040, Oct. 2004.
- [7] Abbou A., Mahmoudi H. and Elbacha A., High-Gain Observer Compensator for Rotor Resistance Variation on Induction Motor RFOC, Proceedings of the 14<sup>th</sup> IEEE International Conference on Electronics, Circuits and Systems, pp.873-877, Marrakech, Morocco, December 11-14, 2007.
- [8] L. Harnefors, K. Pietiläinen, and L. Gertmar, Torque-maximizing field weakening control: Design, analysis, and parameter selection, *IEEE Trans. Ind. Electron.*, vol. 48, no. 1, pp. 161–168, Feb. 2001.
- [9] Tsuji, M., Chen, S., Izumi, K., Yamada, A sensorless vector control system for induction motors using q-axis flux with stator resistance identification, *IEEE Tran. Ind. Electron*, Vol. 48 No.1, pp.476-83.2003.
- [10] N.Teske, G.M.Asher, M.Sumner and K.J. Bradley, Suppression of Effects for the sensorless saturation saliency position control of induction motor drives under loaded condition, *IEEE Tran. On Indus. Electronics*, Vol. 47, No.5, pp. 1142-1149, 2000.
- [11] C. Chakraborty and Y. Hori, Fast Efficiency Optimized Technique for the Indirect Vector Controlled Induction Motor Drives, *IEEE Trans. Ind. Appl.*, Vol.39, pp.1070-1076, July/Aug., 2003.
- [12] M. Boussak, Implementation and experimental investigation of sensorless speed control of permanent magnet synchronous motor drive, *IEEE Transactions on Power Electronics*, vol. 20, n°6, pp. 1413–1422, Nov./Dec. 2005.
- [13] S Mir, M Elbuluk, D Zinger, PI and fuzzy estimators for tuning the stator resistance in direct torque control of induction machines. *IEEE Transactions on Power Electronics*, 13(2): 179-287,1998.
- [14] A. Abbou, H. Mahmoudi and A. Elbacha, Performance of the two strategies of control RFOC and DTFC for induction motor used in electric vehicles, *International Journal Physical and Chemical News*, Vol.44, pp.58-66, 2008.
- [15] M. Bodson, J. Chiasson, A comparison of sensorless speed estimation methods for induction motor control, in: Proceedings of ACC'2002, Anchorage, Alaska, pp. 3076–3081, 2002.
- [16] Hong Wen, Wang Gangge, Nan Tan, AC induction motor direct torque control system with fuzzy controller, *Machine Learning and Cybernetics*, International Conference on, Nov. 2-5, pp.800-802,2003.
- [17] Lascu C., Boldea I., Blaabjerg F., Variable-Structure Direct Torque Control - A Class of Fast and Robust Controllers for Induction Machine Drives. *IEEE Trans. Ind. Electron.*, 2004, 51(4).
- [18] Faiz J., Sharifian M. B. B., Keyhani A., Proca A. B., Sensorless Direct Torque Control of Induction Motors Used in Electric Vehicle. *IEEE Trans. Energy Conv.*, 2003, 18, p. 1-10.
- [19] Lascu C., Boldea I., Blaabjerg F., A Modified Direct Torque Control for Induction Motor Sensorless Drive. *IEEE Trans. Ind. Applicat.*, 2000, 36(1), p. 122-130.
- [20] José R., Jorge P., César S., Samir K., Hemin M., *A Novel Direct Torque Control Scheme for Induction Machines with Space Vector Modulation*. 35th Annual IEEE Power Electron. Specialists Conf. Aachen, Germany, 2004, p. 1392-1397.
- [21] Peresada, S., A. Tilli and A. Tonielli, Indirect stator flux-oriented output feedback control of a doubly fed induction machine. *IEEE Trans. Contr Sys*, 11 (6), 2003, pp: 875-888.